Available online at www.sciencedirect.com
SCIENCE DIRECT
Physics Letters A 355 (2006) 66–72
PHYSICS LETTERS A
www.elsevier.com/locate/pla

Electrical and thermal transport properties of the electron-doped manganites $La_{0.9-x}Y(Ho)_xTe_{0.1}MnO_3$

Gan-Hong Zheng, Yu-Ping Sun *, Xue-Bing Zhu, Wen-Hai Song

Key Laboratory of Materials Physics, Institute of Solid State Physics, Chinese Academy of Sciences, Hefei 230031, PR China

Received 18 October 2005; accepted 31 January 2006

Available online 13 February 2006

Communicated by J. Flouquet

Abstract

Systematical studies of resistivity $\rho(T)$, thermopower $S(T)$, and thermal conduction $\kappa(T)$ have been performed on the electron-doped manganites $La_{0.9-x}A_xTe_{0.1}MnO_3$ (A = Y or Ho, $0.05 \leqslant x \leqslant 0.15$). The Y005, Y010, Ho005 and Ho010 samples exhibit double insulator–metal (I–M) transitions in the $\rho(T)$ curves, one is very close to its Curie temperature T_C, the other is well below T_C. However, the Y015 and Ho015 samples present insulating behaviors in the whole measured temperature. S shows positive sign for all samples with a peak near T_C and a bump/peak in the ferromagnetic (FM) region. The $\rho(T)$ and $S(T)$ data above T_C can be fitted well by the variable-range hopping (VRH) model. The small thermal conduction data suggests that there exists a large JT distortion in the studied samples. Moreover, comparing with the Y-doped compounds, the Ho-doped ones have smaller the thermal conduction value. This result is discussed as the existence of antiferromagnetic (AFM) coupling between Ho and Mn ions in the Ho-doping samples. On the one hand, the magnetic disorder enhancement due to the competition of ferromagnetic (FM) and AFM lower the thermal conductivity, on the other hand, the AFM coupling will reduce the phonon–phonon scattering.

PACS: 75.47.Lx; 75.30.Hx; 75.50.Ee

Keywords: Manganites; Antiferromagnetic coupling; Thermopower; Heat conductivity

1. Introduction

The discovery of colossal magentoresistance (CMR) in the hole-doped manganites has been the subject of intense work for their possible applications such as magnetic reading heads, field sensors and memories [1–3]. Traditionally, the CMR phenomenon is explained by the double-exchange (DE) interaction between Mn^{3+} and Mn^{4+} ions [4]. In addition, the local Jahn–Teller (JT) distortion is also suggested to play a key role in these manganties [5]. Recently, electron-doped compounds in which Ln were substituted by tetravalent ion such as Ce^{4+}, Te^{4+} and Zr^{4+}, etc., have been studied by some research groups [6–8]. These studies indicated that CMR behavior could occur in the system of a mixed-valence state of Mn^{2+} and Mn^{3+}.

The electrical transports $\rho(T)$, thermopower $S(T)$ and thermal conductivity $\kappa(T)$ have been studied extensively for the hole-doped manganites [9–12], however, less attention has been focused on the electron-doped manganites [6]. In this work, we have investigated the electrical transports $\rho(T)$, thermopower $S(T)$, and thermal conductivity $\kappa(T)$ for the electron-doped manganites $La_{0.9-x}A_xTe_{0.1}MnO_3$ (A = Y or Ho, $0.05 \leqslant x \leqslant 0.15$). And the results show that the electronic conduction at high temperatures for all samples is followed by variable-range hopping (VRH) mechanism based on the fitting of the resistivity and thermopower data. The small thermal conduction suggests there exists large JT distortion in the studied samples. Moreover, comparing with the Y-doped manganites, the Ho-doped manganites have smaller the thermal conduction value. This result is discussed as the existence of antiferromagnetic (AFM) coupling between Ho and Mn ions in the Ho-doping samples. On the one hand, the magnetic disorder enhancement due to the competition of ferromagnetic

* Corresponding author. Tel.: +86 551 559 1436; fax: +86 551 559 1434.
E-mail address: ypsun@issp.ac.cn (Y.-P. Sun).

0375-9601/$ – see front matter
doi:10.1016/j.physleta.2006.01.095

(FM) and AFM lower the thermal conductivity, on the other hand, the AFM coupling will reduce the phonon–phonon scattering.

2. Experimental

Polycrystalline samples with nominal compositions $La_{0.9-x}A_xTe_{0.1}MnO_3$ where A = Y and Ho ($x = 0.05$, 0.10 and 0.15, which are referred to as Y005, Y010, Y015, Ho005, Ho010 and Ho015 below) were prepared by solid-state reaction method. Stoichiometric high-purity La_2O_3, Y_2O_3(Ho_2O_3), TeO_2 and MnO_2 powders were mixed and ground, and then heated in air at 750 °C for 24 h. The powder obtained was ground, pelletized, and sintered at 1100 °C for 24 h with three intermediate grinding, and finally, the furnace was cooled down to the room temperature. The structure and lattice constant were determined by powder X-ray diffraction using Cu K_a radiation at the room temperature. The resistance was measured by the standard four-probe method from 5 to 350 K. The thermopower and thermal conductivity were measured in a commercial physical property measurement system (PPMS, $1.8 \leqslant T \leqslant 400$ K, $0 \leqslant H \leqslant 9$ T) from 5 to 350 K.

3. Results and discussion

3.1. X-ray diffraction

Fig. 1(a) shows the XRD pattern of $La_{0.9-x}Y(Ho)_xTe_{0.1}MnO_3$ ($x = 0.05$, 0.10 and 0.15) samples. It can be found that all samples are single phase with no detectable secondary phases. XRD patterns for all samples can be indexed by rhombohedral lattice with the space group $R\bar{3}C$, and we present experimental and calculated XRD patterns for the Ho015 sample in Fig. 1(b). It can be seen that the fitting between the experimental spectra and calculated values is relatively good. The structural parameters are refined by the standard Rietveld technique and the fitting between the experimental spectra and the calculated values are shown in Table 1.

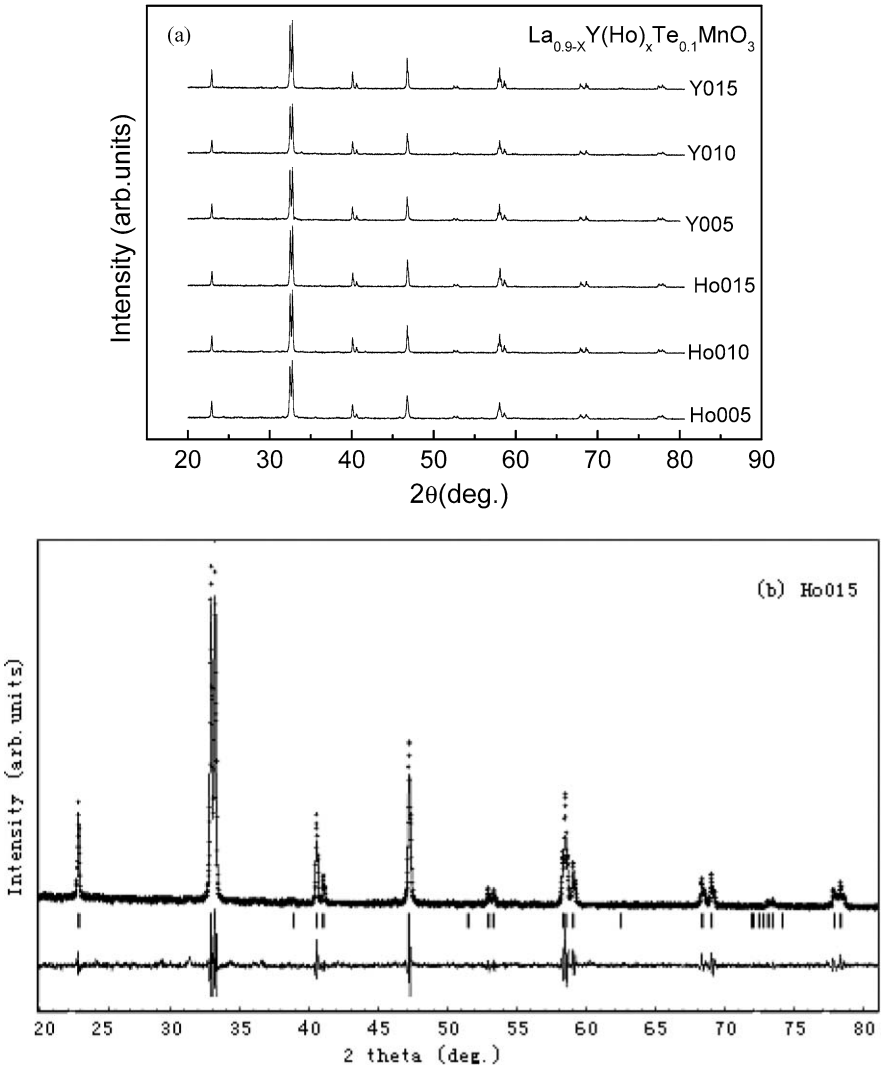

Fig. 1. (a) XRD patterns of the compound $La_{0.9-x}Y(Ho)_xTe_{0.1}MnO_3$ ($x = 0.05$, 0.10, 0.15). (b) The experimental and calculated XRD patterns of the compound Ho015. Crosses indicate the experimental data and the calculated data is continuous line overlapping them. The lowest curve shows the difference between experimental and calculated patterns. The vertical bars indicated the expected reflection positions.